Available online at www.sciencedirect.com

ELSEVIER

Journal of Catalysis 222 (2004) 307–314

JOURNAL OF CATALYSIS

www.elsevier.com/locate/jcat

Flame spray synthesis of Pd/Al_2O_3 catalysts and their behavior in enantioselective hydrogenation

Reto Strobel,[a,b] Frank Krumeich,[c] Wendelin J. Stark,[a,b] Sotiris E. Pratsinis,[a] and Alfons Baiker[b,*]

[a] *Particle Technology Laboratory, Department of Mechanical and Process Engineering, ETH Zentrum, CH-8092 Zürich, Switzerland*
[b] *Institute for Chemical- and Bioengineering, Department of Chemistry, ETH Hönggerberg, CH-8093 Zürich, Switzerland*
[c] *Laboratory of Inorganic Chemistry, Department of Chemistry, ETH Hönggerberg, CH-8093 Zürich, Switzerland*

Received 6 August 2003; revised 8 October 2003; accepted 23 October 2003

Abstract

Flame spray pyrolysis (FSP) was used for the synthesis of alumina-supported palladium catalysts containing 1–7.5 wt% Pd. Precursor solutions of aluminum *sec*-butoxide and palladium acetylacetonate were sprayed and combusted, resulting in nanostructured materials that were characterized by high-resolution transmission electron microscopy, CO-pulse chemisorption, nitrogen adsorption, and X-ray diffraction. Well-dispersed palladium particles (1–5 nm) were confined to the alumina surface. Palladium dispersion depended on the metal loading and decreased for higher amounts of Pd. The FSP-derived alumina-supported palladium catalysts were chirally modified with cinchonine and tested for the enantioselective hydrogenation of 4-methoxy-6-methyl-2-pyrone. Rate and enantioselectivity decreased with higher Pd dispersion. A comparison of these catalysts to a corresponding commercial Pd/Al_2O_3 catalyst revealed lower reaction rate and enantioselectivity for the FSP-derived catalysts. However, hydrogen pretreatment of the flame-made catalysts at 500 °C improved rate and enantioselectivity strongly, whereas only a comparatively weak beneficial effect was observed with the corresponding wet-phase-derived catalysts. Enantiomeric excess in the formation of (*R*)-4-methoxy-6-methyl-5,6-dihydro-2-pyrone reached 80% for flame-made catalysts after pretreatment in hydrogen. Hydrogen pretreatment temperatures above 600 °C led to sintering of the Pd particles and drastic loss in activity and enantioselectivity.

Keywords: Flame spray pyrolysis; Palladium; Alumina; Hydrogenation; Methoxypyrone; Chiral; Enantioselective; Asymmetric; PACS

1. Introduction

Most noble-metal-based catalysts consist of nanometer-sized metal particles dispersed on high-surface-area supports [1]. Flame synthesis is a relatively new method for the one-step production of supported noble metal catalysts and catalysts in general [2,3]. Moser et al. [4] made noble metal nanoparticles supported on Al_2O_3 of low specific surface area (10 $m^2\,g^{-1}$) by a high-temperature decomposition process. Johannessen and Koutsopoulos [5] prepared Pt/TiO_2 catalysts for SO_2 oxidation using a vapor-fed aerosol flame reactor. Since their platinum precursor showed very low volatility they operated at very low production rates (some $mg\,h^{-1}$). Very recently, Jensen et al. [6] reported the flame aerosol synthesis of $Cu/ZnO/Al_2O_3$ catalysts for methanol synthesis. In contrast to the aerosol route, flame spray pyrolysis offers the possibility of using nonvolatile precursors and was applied for synthesis of Pt/Al_2O_3 hydrogenation catalysts [7] at a considerably higher production rate of 15 $g\,h^{-1}$ and Au supported on TiO_2 and SiO_2 [8].

Flame aerosol synthesis is used on a large scale today to produce carbon black, fumed silica, and titania pigments. Flame synthesis in general and especially flame spray pyrolysis is a fast, cost-effective, and versatile process for the production of a wide variety of different nanoparticles [9–11]. More specifically, in this process a flame is used to drive chemical reactions of precursor compounds, resulting in the formation of clusters, which grow to nanometer-sized products by coagulation and sintering [10].

In the field of fine chemical synthesis, palladium is one of the most versatile and most widely applied catalytic metals [12]. Heterogeneous enantioselective hydrogenation over platinum catalysts, chirally modified by cinchona alkaloids and derivatives, has been intensively investigated and cov-

---

[*] Corresponding author.
E-mail address: baiker@tech.chem.ethz.ch (A. Baiker).

0021-9517/$ – see front matter © 2003 Elsevier Inc. All rights reserved.
doi:10.1016/j.jcat.2003.10.012

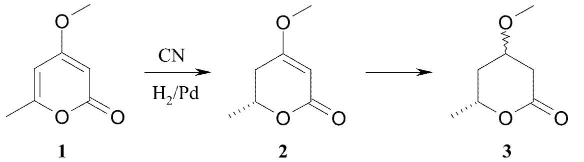

Scheme 1. Hydrogenation of 4-methoxy-6-methyl-2-pyrone **1** over cinchona-modified palladium; **2**, (R)-4-methoxy-6-methyl-5,6-dihydro-2-pyrone; **3**, 4-methoxy-6-methyl-tetrahydro-2-pyrone.

ered in several recent reviews [13–18]. Less effort was spent on the study of analogous palladium systems [16,17]. Since the first report on the Pd-cinchona-catalyzed hydrogenation of a C=C bond in 1985 [19], systematic investigations focused on α,β-unsaturated acids and ketons. Enantiomeric excess (ee) is usually low or moderate with exception of the Pd-cinchona-catalyzed hydrogenation of hydroxy- and methoxymethylpyrone [20,21]. Dihydropyrones are important chiral intermediates in the synthesis of biologically active compounds [22]. At present, the most widely used Pd catalysts for heterogeneous enantioselective hydrogenation are Pd/Al_2O_3 [23] and Pd/TiO_2 [20] but also Pd on Fe_2O_3 [24] and other materials [25] have been used.

Flame synthesis offers the possibility of synthesizing nonporous catalysts with high specific surface area, providing high accessibility for reactants and chiral modifiers [7]. This prompted us to synthesize Pd/Al_2O_3 catalysts by flame spray pyrolysis and test them for the enantioselective hydrogenation of 4-methoxy-6-methyl-2-pyrone (Scheme 1). The catalytic behavior of the new flame-made catalysts will be compared to that of state-of-the-art reference catalysts.

2. Experimental

2.1. Particle synthesis

Fig. 1 shows the experimental setup for the synthesis of Pd/Al_2O_3 by flame spray pyrolysis. Precursor solutions were prepared by dissolving appropriate amounts of aluminum *sec*-butoxide ($Al(s\text{-}BuO)_3$, Aldrich, 97%) and palladium acetylacetonate ($Pd(acac)_2$, Strem, 99%) in xylene (Riedel deHaen, 96%)/acetonitrile (Fluka, 99.5%) mixtures (70/30 vol%). The aluminum concentration was always 0.675 M. In a typical run, the liquid precursor mixture was fed in the center of a methane/oxygen flame by a syringe pump (Inotech) and dispersed by oxygen (3 ml min^{-1}), forming a fine spray. The pressure drop at the capillary tip was kept constant at 1.5 bar by adjusting the orifice gap area at the nozzle. The spray flame was surrounded and ignited by a small flame ring issuing from an annular gap (0.15 mm spacing, at a radius of 6 mm). The total gas flow rate through this premixed methane/oxygen-supporting flame ring was 3.5 L min^{-1} with a fuel/oxygen ratio of 0.92. A sintered metal plate ring (8 mm wide, starting at a radius of 8 mm) provided an additional sheath flow surrounding the spray flame. Calibrated mass-flow controllers (Bronkhorst) were used to monitor all gas flows. Product particles were collected on a glass fiber filter (Whatmann GF/A, 15 cm in diameter) with the aid of a vacuum pump.

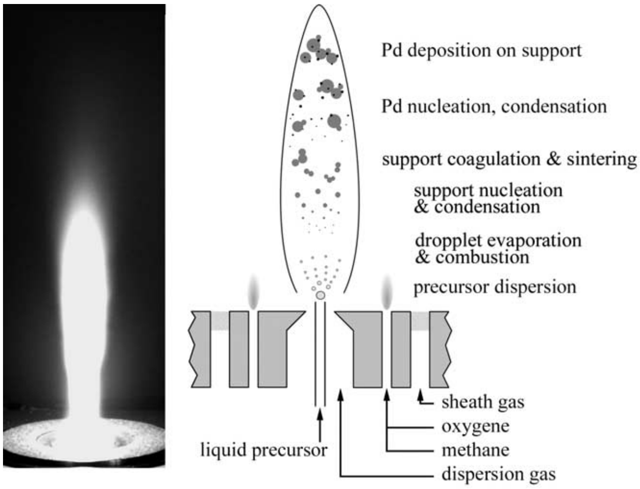

Fig. 1. Sketch of the flame spray pyrolysis unit. The liquid precursor mixture is rapidly dispersed by a gas stream and ignited by a premixed methane/oxygene flame. After evaporation and burning of the precursor, particles are formed by nucleation, condensation, coalescence, and coagulation. The image shows a typical spray flame producing Pd/Al_2O_3 nanoparticles.

For some catalysis experiments, the flame-made and reference catalysts were subjected to a heat pretreatment in flowing hydrogen. The samples, placed in a U-tube, were flushed by He (20 ml min^{-1}) for 20 min and then pretreated by heating at 10 °C min^{-1} in flowing hydrogen (20 ml min^{-1}) up to a certain temperature (100–800 °C) and kept constant at this temperature for 1 h.

As reference materials a 5 wt% Pd/TiO_2 prepared by wet precipitation [20] and a commercial 5 wt% Pd/Al_2O_3 catalyst (Engelhard 40692) were used. Characteristic properties of these catalysts are listed in Table 1.

2.2. Catalyst characterization

The specific surface area (SSA) of the as-prepared powders was determined by nitrogen adsorption at 77 K using the BET method (Micromeritics Tristar). All samples were outgassed at 150 °C for 1 h prior to analysis. The pore-size distribution was determined from the desorption branch of a fully recorded isotherm of the as-prepared powders (Micromeritics ASAP 2010 Multigas System). The powder X-ray diffraction pattern was recorded with a Bruker D8 advance diffractometer from 20 to 65°, step size 0.06°, at a scan speed of 0.72° min^{-1}.

For transmission electron microscopy (TEM), the material was dispersed in ethanol and deposited onto a perforated carbon foil supported on a copper grid. The investigations were performed on a Tecanai 30F microscope (Philips; field emission cathode, operated at 300 kV). The high-resolution TEM (HRTEM) images were recorded on a slow-scan CCD camera. Scanning transmission electron

Table 1
Catalytic behavior and structural properties of flame-made 5 wt% Pd/Al_2O_3 and reference catalysts

No.	Sample	Pretreatment	BET SSA ($m^2\,g^{-1}$)	Pd dispersion[a] (%)	Pd diameter (nm)	TOF[b] (min^{-1})	r_0 ($mol\,kg_{Pd}^{-1}\,min^{-1}$)	Selectivity[c] (%)	ee (%)
1	5% Pd/Al_2O_3 N_2 disp.	None	115	26	4.3	0.59	1.38	80	60
2	5% Pd/Al_2O_3 air disp.	None	108	24	4.7	0.55	1.24	81	60
3	5% Pd/Al_2O_3 N_2 sheath	None	127	30	3.7	0.42	1.18	77	57
4	5% Pd/Al_2O_3 air sheath	None	121	28	4.0	0.47	1.23	77	60
5	5% Pd/Al_2O_3 1 ml liquid feed	None	197	39	2.8	0.12	0.44	–	40[d]
6	5% Pd/Al_2O_3 6 ml liquid feed	None	73	19	5.8	0.65	1.17	82	60
7	5% Pd/Al_2O_3 standard conditions	None	120	27	4.1	0.42	1.06	81	57
8	5% Pd/Al_2O_3 standard conditions	1 h 500 °C H_2		26	4.3	1.63	**3.97**	**91**	**80**
9	5% Pd/Al_2O_3 (E40692)	None	205	29	3.9	0.69	1.88	84	66
10	5% Pd/Al_2O_3 (E40692)	1 h 400 °C H_2		29	3.9	0.97	2.63	88	67
11	5% Pd/TiO_2[e]	None	57	22	5.0	1.35	2.79	81	73
12	5% Pd/TiO_2[e]	1 h 400 °C H_2		21	5.3	0.66	**1.31**	**84**	**74**

[a] Determined by CO-pulse chemisorption.
[b] TOF is given per Pd surface atoms, as determined by CO-pulse chemisorption.
[c] Chemoselectivity: Amount of **2** related to the total amount of **2** and **3** (Scheme 1).
[d] Determined at 20% conversion.
[e] Prepared according to recipe given in [20].

microscopy (STEM) images, obtained with a high-angle annular dark-field (HAADF) detector, show the metal particles with bright contrast (Z contrast). The Sauter-mean diameter (d_S) of the Pd particle-size distribution as derived from STEM-images was calculated according to

$$d_S = \frac{\sum n_i d_i^3}{\sum n_i d_i^2}.$$

Palladium dispersion was determined by CO-pulse chemisorption at 35 °C using a He flow of 50 $ml\,min^{-1}$ and pulses of 0.5 ml (10% CO in He) on a Micromeritics Autochem II 2920 unit. Prior to experiment all samples were freshly reduced for 1 h at 250 °C under flowing hydrogen (20 $ml\,min^{-1}$) and then flushed by He (50 $ml\,min^{-1}$) at 260 °C for 90 min. In order to calculate the metal dispersion, an adsorption stoichiometry of $Pd/CO = 1$ was assumed [26].

2.3. Catalytic measurements

The hydrogenation reactions were carried out in a magnetically stirred 100-ml glass reactor. In the standard procedure 20 mg catalyst in 10 ml 2-propanol (Fluka, 99.8%) was pretreated in situ under flowing hydrogen for 5 min at 1 bar and room temperature. One milligram of cinchonine (CN, Fluka, 98%) was added and after 5 min stirring the reaction was started by addition of 50 mg 4-methoxy-6-methyl-2-pyrone **1** (Aldrich, purified by sublimation in vacuum, followed by recrystallization from n-hexane) [20]. As shown earlier by Künzle et al. [27] external mass transfer is not an issue for this relatively slow reaction.

Conversion, chemoselectivity (Scheme 1, amount of **2** related to the total amount of **2** and **3**), and enantiomeric excess ($ee(\%) = |R(\%) - S(\%)|$) were determined by chromatographic analysis using a Chrompack Chirasil-DEX CB column. Using cinchonine as chiral modifier afforded excess of the (R)-enantiomer. If not otherwise stated, enantioselectivity and chemoselectivity were determined at 50% conversion.

3. Results

3.1. Catalyst properties

Flame spray pyrolysis (FSP) of the palladium/alumina precursor solutions resulted in spherical alumina particles in the size range of 10–30 nm with well dispersed palladium particles attached to the surface (Fig. 2). Different Pd/Al_2O_3 powders containing 0–7.5 wt% Pd were produced using the same flame conditions (liquid feed rate, 3 $ml\,min^{-1}$; O_2 dispersion gas flow rate, 3 $L\,min^{-1}$) and for selected 5 wt% Pd under different flame conditions (sheath gas, 20 $L\,min^{-1}$ O_2, air, or N_2; dispersion gas, 3 $ml\,min^{-1}$ O_2, air, or N_2). XRD measurements revealed small γ-alumina crystals for all flame-made powders giving rise to some line broadening. Adding Pd had no influence on BET-SSA and alumina crystal structure as determined by XRD.

Table 1 gives an overview of structural and catalytic properties of different FSP-derived materials and two standard reference catalysts (entries 9–12). Using standard conditions the specific surface area of FSP-derived Pd/Al_2O_3 was about 120 $m^2\,g^{-1}$. Changing the dispersion or sheath gas from O_2 to air or N_2 had only little influence on specific surface area and Pd dispersion. However, varying the liquid flow rate from 6 to 1 $ml\,min^{-1}$ resulted in specific surface areas ranging from about 70 to 200 $m^2\,g^{-1}$.

Fig. 2 shows an STEM image of the flame-made Pd/Al_2O_3 catalyst. The palladium particles, with a diameter of 1 to 5 nm, are confined to the alumina surface, and "uniformly" dispersed. The mass-based palladium particle-size distribution derived from STEM images is rather narrow with

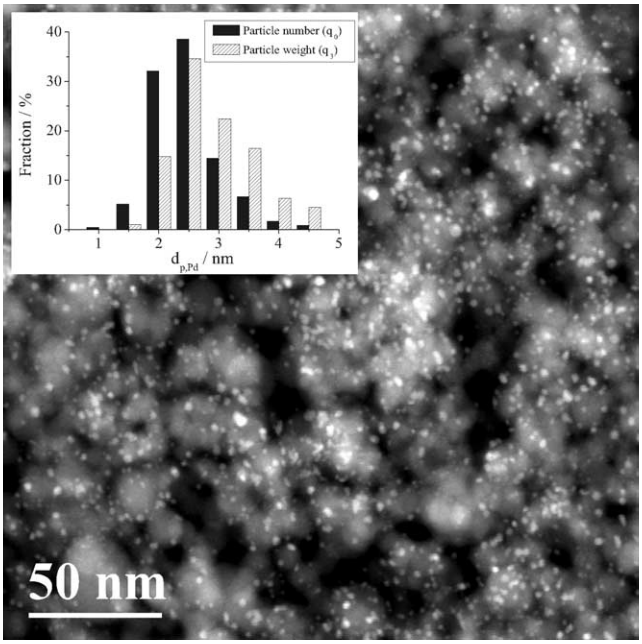

Fig. 2. Scanning transmission electron microscopy (STEM) picture of flame-made Pd/Al_2O_3 prepared under standard conditions. Small Pd particles (1–5 nm) are well dispersed and confined to the alumina surface. The inset shows the corresponding Pd particle-size distribution of 500 counted particles with a Sauter mean diameter $d_S = 2.7$ nm and the mass-based geometric standard deviation $\sigma_{g,3} = 1.3$.

geometric standard deviation $\sigma_{g,3} = 1.3$ and Sauter mean diameter $d_S = 2.7$ nm.

Fig. 3 shows high-resolution transmission electron microscopy images. As-prepared (A) and hydrogen-treated (B, 500 °C; C, 700 °C) 5 wt% Pd/Al_2O_3 powders indicate crystalline palladium for all samples. The Pd particle size seemed to increase after pretreatment at 700 °C in flowing hydrogen. For the sample pretreated at 500 °C, the Pd particle size did not change compared to the unpretreated, as-prepared material.

The influence of pretreatment temperature (1 h under flowing hydrogen) on the dispersion is shown in Fig. 4. The Pd dispersion stays virtually constant up to 600 °C and decreases at higher pretreatment temperatures (from 28% at 600 °C down to 8% at 800 °C) as the Pd particle size increases.

Pore-size distributions of a typical flame-made powder and the reference catalysts are shown in Fig. 5. The FSP-derived material and the Pd/TiO_2 reference are nonporous, whereas the commercial standard catalyst (E40692) is a mesoporous material.

3.2. Enantioselective hydrogenation

As-prepared materials were tested for the enantioselective hydrogenation of 4-methoxy-6-methyl-2-pyrone using cinchonine as chiral modifier (Scheme 1). This modifier affords the (R)-4-methoxy-6-methyl-5,6-dihydro-2-pyrone (**2**) as major enantiomer (Scheme 1). Fig. 6 shows the typical dependence of enantioselectivity and chemoselectivity on conversion. Chemoselectivity decreased with higher conversion while ee was virtually unaffected. This behavior was observed for all flame-made materials as well as for the reference catalysts. Fig. 7 depicts enantioselectivity and turnover frequency (TOF) as a function of palladium dispersion of flame-made catalysts with 1–7.5 wt% Pd prepared at standard conditions and 5 wt% Pd produced with different liquid flow rates (1–6 $\mathrm{ml\,min^{-1}}$). Enantiomeric excess as well as activity decreased with higher metal dispersion. Fig. 8 shows the catalytic performance as a function of the hydrogen pretreatment temperature of the catalyst. The performance in terms of activity, enantioselectivity, and chemoselectivity increased up to a pretreatment temperature of 500–600 °C and decreased for higher temperatures.

Table 1 gives an overview of catalytic data of different FSP-derived materials and the reference catalysts (entries 9–12). Catalysts were tested either as-prepared or after a heat pretreatment under flowing hydrogen. Using different sheath or dispersion gases (O_2, air, or N_2) for the flame synthesis of Pd/Al_2O_3 had only slight influence on the catalytic performance (entries 1–4). Note that the flame-made catalysts with similar dispersion (entry 7) as the two reference catalysts (entries 9 and 11) showed lower enantioselectivity and rate. However, the hydrogen pretreatment increased turnover frequency, chemoselectivity, and enantioselectivity to (R)-4-methoxy-6-methyl-5,6-dihydro-2-pyrone formation for the flame-made powder (from 57 up to 80% ee), whereas the corresponding properties of the reference catalysts were much less improved (entries 9 and 10). Turnover frequency increased for alumina-supported catalysts (flame-made and E40692), whereas it decreased for the pretreated Pd/TiO_2 reference.

4. Discussion

4.1. Catalyst properties

The alumina support of Pd/Al_2O_3 made by flame spray pyrolysis mainly consists of spherical, poorly crystalline γ-alumina particles, as previously observed for flame-made alumina [10]. Adding palladium did not affect the morphology or crystallinity of the alumina support, consistent with an earlier study on Pt/alumina [7]. Changing the flame conditions by applying different dispersion or sheath gases (O_2, air, N_2) did not have a major effect on the morphology of the alumina support or the Pd particles. These flame conditions with different sheath and dispersion gases resulted in similar flame heights, indicating similar particle residence times at high temperature, where particles grow by coagulation and sintering. However, changing the precursor flow rate alters the enthalpy content of the flame that results in different residence times at high temperature and, consequently, particles with different size and specific surface area ranging from 73 to 197 $\mathrm{m^2\,g^{-1}}$ (Table 1). This is consistent with flame spray synthesis of alumina and other oxides [7,28].

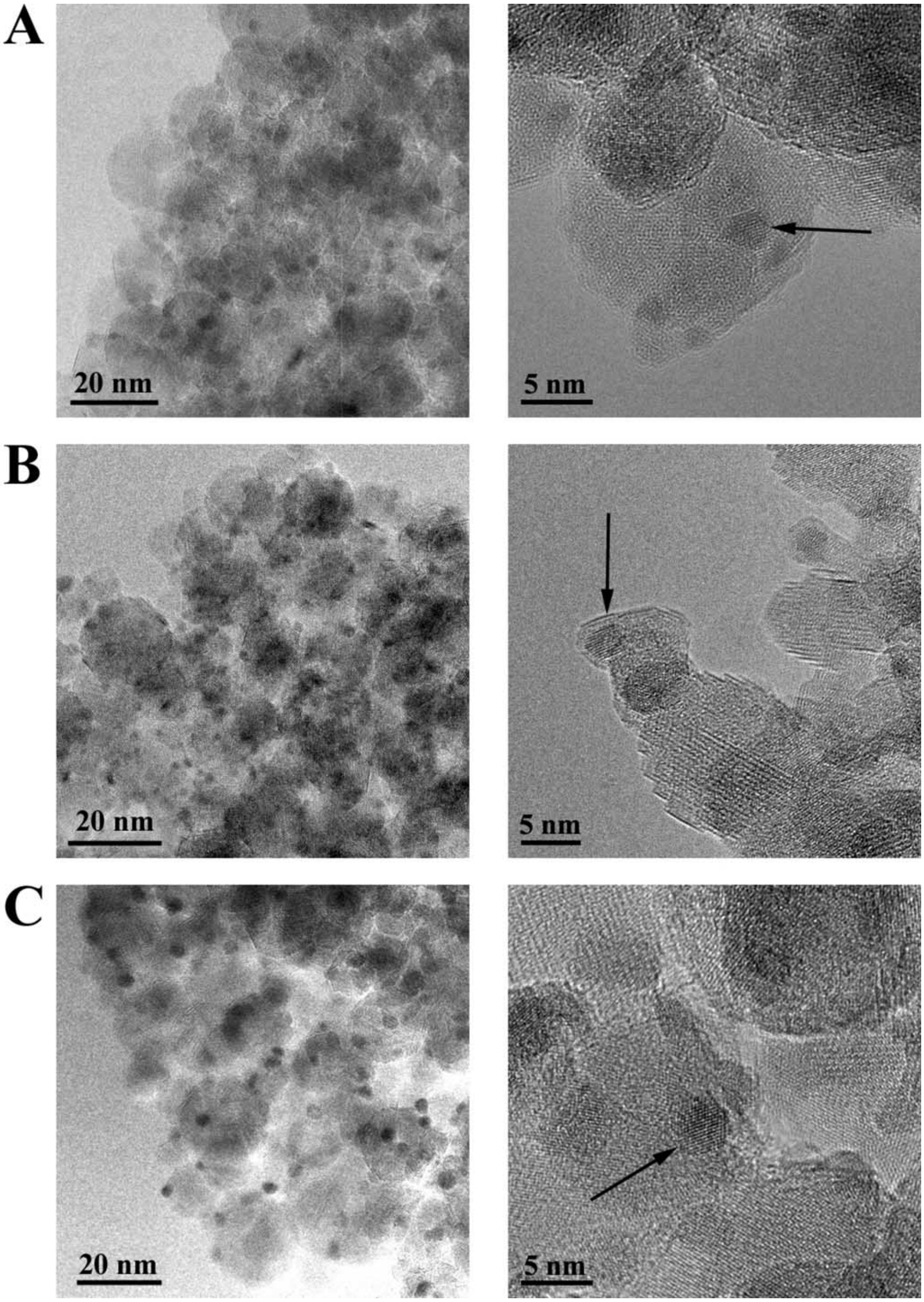

Fig. 3. HRTEM pictures of 5 wt% Pd/Al_2O_3 made by flame spray pyrolysis. (A) As prepared; and after pretreatment in flowing hydrogen at (B) 500 °C and (C) 700 °C. Pictures with higher magnification on the right-hand side depict the corresponding crystalline Pd particles with lattice planes.

Palladium forms small particles on the alumina surface ranging from 1 to 5 nm in diameter with a narrow size distribution (Fig. 2), similar to supported platinum catalysts made in vapor- or liquid-fed flames [5,7]. In general, higher palladium loadings, achieved by increasing the Pd content or decreasing the alumina surface area, lead to larger metal particles and thus lower dispersion.

The particle formation process of alumina-supported palladium is illustrated in Fig. 1. Alumina has a much lower vapor pressure than Pd/PdO in the hot flame environment, and consequently alumina particle formation starts earlier. Further downstream the flame, at lower temperatures, Pd/PdO starts to form small particles and/or deposits directly on the alumina support. This particle formation mechanism was also suggested for Pt/TiO_2 [5] and Pt/Al_2O_3 [7].

Hydrogen treatment up to 600 °C of FSP-derived Pd/Al_2O_3 has no significant influence on metal dispersion, indicating high thermal stability of these catalysts. However, at

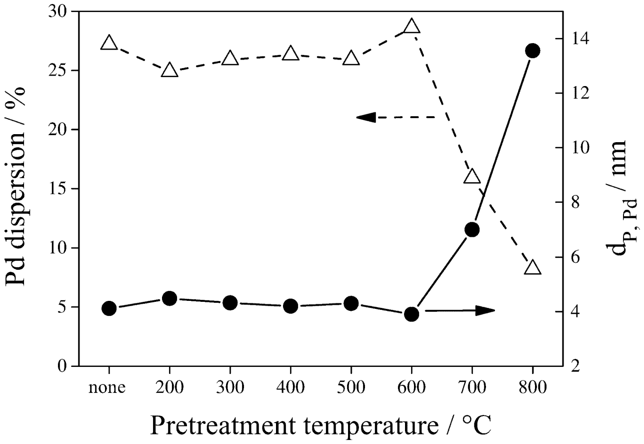

Fig. 4. Palladium dispersion and calculated Pd particle diameter ($d_{P,Pd}$) as a function of pretreatment temperature under flowing hydrogen for 1 h.

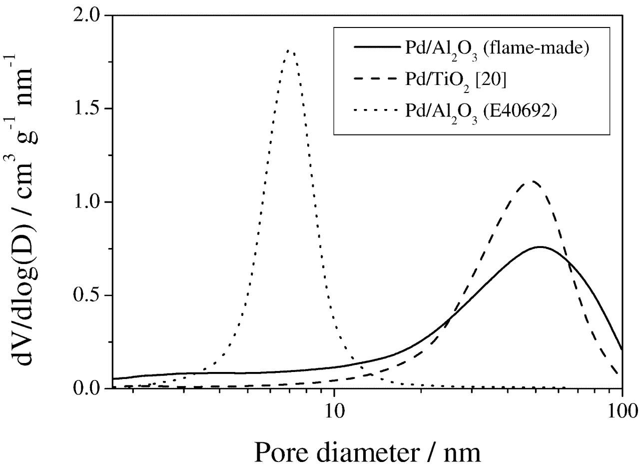

Fig. 5. Pore-size distribution as determined from the nitrogen desorption isotherm of a typical flame-made Pd/Al_2O_3 powder, a precipitated Pd/TiO_2 [20], and a commercial Pd/Al_2O_3 catalyst (E40692).

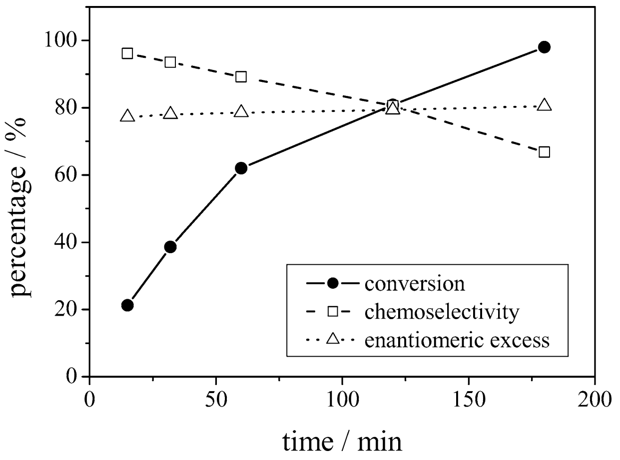

Fig. 6. Typical behavior of chemoselectivity and ee of flame-made Pd/Al_2O_3 catalysts as a function of conversion (entry No. 8, Table 1).

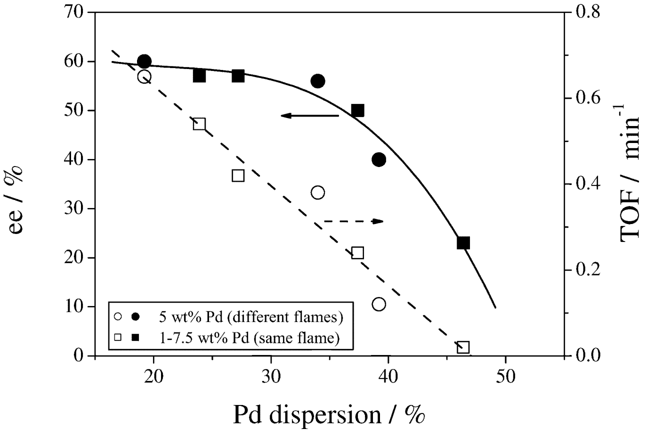

Fig. 7. Enantiomeric excess (ee) and turnover frequency (TOF) as a function of Pd dispersion of flame-made catalysts containing 1–7.5 and 5 wt% Pd produced under standard conditions and varying liquid flow rate (1–6 ml min^{-1}), respectively.

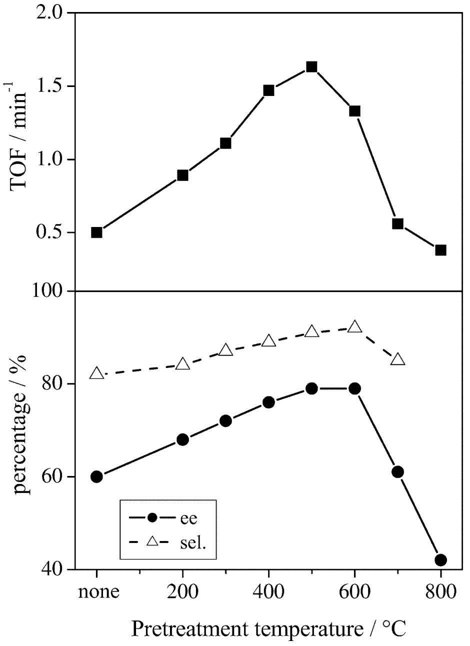

Fig. 8. Catalytic performance of a FSP-derived 5 wt% Pd/Al_2O_3 catalyst as a function of pretreatment temperature for 1 h under flowing hydrogen.

higher temperatures palladium starts sintering as indicated by a drop in dispersion, i.e., from 28% at 600 °C down to 8% at 800 °C (Fig. 4). This sintering behavior above 600 °C was also observed in a model study [29]. Closer inspection of the HRTEM images (Fig. 3) indicates an enhanced formation of facetted palladium as a result of the hydrogen treatment at 500 °C.

4.2. Enantioselective hydrogenation

Flame-made Pd/Al_2O_3 chirally modified by cinchonine is a suitable catalyst for the enantioselective hydrogenation of 4-methoxy-6-methyl-2-pyrone to (*R*)-4-methoxy-6-methyl-5,6-dihydro-2-pyrone (**2**), in terms of activity, chemo-, and enantioselectivity. Considerable improvement of the properties is achieved after pretreatment of the flame-made material in flowing hydrogen at elevated temperatures. After this pretreatment the flame-made materials show similar enantioselectivity and turnover frequency as the best known catalyst (5 wt% Pd/TiO_2) for this reaction [20] and better performance than an often used commercial Pd/Al_2O_3 catalyst (Table 1). Interestingly the hydrogen pretreatment has a much stronger positive effect on the catalytic properties for the flame-made Pd/Al_2O_3 catalyst, whereas its effect on the Pd/TiO_2 reference catalyst is even negative, corroborating earlier studies [21].

The degree of Pd dispersion affects the catalytic performance remarkably (Fig. 7). TOF decreases with increasing metal dispersion and a significant drop in enantioselectivity is observed for catalysts with Pd dispersion higher than about 35%. Nitta et al. [30] observed a similar dependence of metal dispersion of Pd/TiO_2 catalysts for the enantioselective hydrogenation of phenylcinnamic acid. This indicates that the reaction is structure sensitive and small palladium particles result in lower enantioselectivity and turnover frequencies. An earlier study on flame-made Pt/Al_2O_3 revealed a similar dependence on metal loading for the enantioselective hydrogenation of ethyl pyruvate [7].

For the flame-made catalysts, activity, chemoselectivity, and enantioselectivity increased continuously up to a pretreatment temperature of about 500 °C and decreased rapidly for temperatures above 600 °C (Fig. 8). Nitta et al. [30] reported a similar behavior for Pd/TiO_2 concerning the enantioselectivity; however, the catalytic activity behaved differently and decreased already after pretreatment in hydrogen at low temperatures. The steep decrease in activity can be explained by the sintering of palladium above 600 °C (Fig. 4), resulting in much smaller palladium surface area that is accessible for catalysis. Possible reasons for the increase of the catalytic performance after hydrogen pretreatment are cleaning (decontamination) and/or restructuring of the alumina support and the Pd surface, resulting in a smooth surface exposing mainly thermodynamically more stable low index planes. Some evidence for palladium surface restructuring emerges from the HRTEM images (Fig. 3), indicating more facetted palladium particles after heat pretreatment in hydrogen. It should be noted that an increase of the catalytic performance after heat pretreatment in hydrogen is commonly observed for enantioselective hydrogenation with cinchona-modified Pt/alumina catalysts [31]. The effect of the hydrogen pretreatment at higher temperature is however not understood yet on the atomic level and requires further studies on well-defined single crystal palladium surfaces.

5. Conclusions

The flame spray pyrolysis method has been successfully applied for the synthesis of Pd/Al_2O_3 hydrogenation catalysts. Materials with good catalytic performance in the enantioselective hydrogenation of 4-methoxy-6-methyl-2-pyrone could be produced in a single-step flame synthesis process. The catalysts are made up of small palladium particles (1–5 nm) attached to the surface of agglomerated, nonporous alumina particles (10–30 nm) and exhibit high thermal stability. Hydrogen pretreatment at elevated temperatures improved drastically the catalytic properties (TOF, ee, chemoselectivity) of flame-made catalysts in the hydrogenation of 4-methoxy-6-methyl-2-pyrone. After pretreatment flame-made catalysts showed a higher rate and enantioselectivity than reference catalysts prepared by conventional methods. The flame-made catalysts with different Pd particle sizes revealed a significant structure sensitivity of the reaction.

Acknowledgments

Financial support by the Swiss Commission for Technology and Innovation (KTI) and the Swiss Federal Institute of Technology (ETH) is kindly acknowledged.

References

[1] A.T. Bell, Science 299 (2003) 1688.
[2] W.J. Stark, S.E. Pratsinis, A. Baiker, Chimia 56 (2002) 485.
[3] W.J. Stark, S.E. Pratsinis, Powder Technol. 126 (2002) 103.
[4] W.R. Moser, J.A. Knapton, C.C. Koslowski, J.R. Rozak, R.H. Vezis, Catal. Today 21 (1994) 157.
[5] T. Johannessen, S. Koutsopoulos, J. Catal. 205 (2002) 404.
[6] J.R. Jensen, T. Johannessen, S. Wedel, H. Livbjerg, J. Catal. 218 (2003) 67.
[7] R. Strobel, W.J. Stark, L. Mädler, S.E. Pratsinis, A. Baiker, J. Catal. 213 (2003) 296.
[8] L. Mädler, W.J. Stark, S.E. Pratsinis, J. Mater. Res. 18 (2003) 115.
[9] H.K. Kammler, L. Mädler, S.E. Pratsinis, Chem. Eng. Technol. 24 (2001) 583.
[10] S.E. Pratsinis, Prog. Energy Combust. Sci. 24 (1998) 197.
[11] M.S. Wooldridge, Prog. Energy Combust. Sci. 24 (1998) 63.
[12] H.U. Blaser, A. Indolese, A. Schnyder, H. Steiner, M. Studer, J. Mol. Catal. A 173 (2001) 3.
[13] A. Baiker, H.U. Blaser, in: G. Ertl, H. Knözinger, J. Weitkamp (Eds.), Handbook of Heterogeneous Catalysis, Vol. 5, VCH, Weinheim, 1997, p. 2422.
[14] A. Baiker, J. Mol. Catal. A 115 (1997) 473.
[15] A. Baiker, J. Mol. Catal. A 163 (2000) 205.
[16] M. Studer, H.U. Blaser, C. Exner, Adv. Synth. Catal. 345 (2003) 45.
[17] T. Mallat, A. Baiker, in: R.A. Sheldon, H. van Bekkum (Eds.), Fine Chemicals through Heterogeneous Catalysis, Wiley–VCH, Weinheim, 2001.
[18] P.B. Wells, A.G. Wilkinson, Top. Catal. 5 (1998) 39.
[19] J.R.G. Perez, J. Malthete, J. Jacques, C. R. Acad. Sci. II 300 (1985) 169.
[20] W.R. Huck, T. Bürgi, T. Mallat, A. Baiker, J. Catal. 200 (2001) 171.
[21] W.R. Huck, T. Mallat, A. Baiker, Catal. Lett. 80 (2002) 87.
[22] K.R. Romines, J.K. Morris, W.J. Howe, P.K. Tomich, M.M. Horng, K.T. Chong, R.R. Hinshaw, D.J. Anderson, J.W. Strohbach, S.R. Turner, S.A. Mizsak, J. Med. Chem. 39 (1996) 4125.
[23] K. Borszeky, T. Mallat, A. Baiker, Tetrahedron: Asymm. 8 (1997) 3745.

[24] H.Z. Ma, B. Wang, Q.Z. Shi, Synth. Commun. 33 (2003) 175.
[25] I. Kun, B. Török, K. Felföldi, M. Bartòk, Appl. Catal. A 203 (2000) 71.
[26] J.R. Anderson, Structure of Metallic Catalysts, Academic Press, London, 1975.
[27] N. Künzle, J.W. Soler, T. Mallat, A. Baiker, J. Catal. 210 (2002) 466–470.
[28] L. Mädler, H.K. Kammler, R. Mueller, S.E. Pratsinis, J. Aerosol. Sci. 33 (2002) 369.
[29] J.J. Chen, E. Ruckenstein, J. Catal. 69 (1981) 254.
[30] Y. Nitta, T. Kubota, Y. Okamoto, Bull. Chem. Soc. Jpn. 73 (2000) 2635.
[31] H.U. Blaser, H.P. Jalett, D.M. Monti, A. Baiker, J.T. Wehrli, Stud. Surf. Sci. Catal. 67 (1991) 147.